values of $P(v)$ obtained in this manner were compared with the initial ones.

[4)]The ordinate scales in Figs. 3 and 4 are the same for the H and D atoms. The relative values were chosen such that the total area under the $P(E)$ curve was proportional to the excitation cross sections of the corresponding hydrogen and deuterium lines. The values of the cross section were taken from[10].

[5)]The symbol $n'$ is used for the principal quantum number of the Rydberg state to distinguish it from the principal quantum number $n$ of the excited dissociation fragments.


[1]R. S. Freund, J. A. Schiavone, and D. F. Brader, J. Chem. Phys. **64**, 1122 (1976).
[2]G. N. Polyakova, V. F. Erko, A. I. Ranyuk, and O. S. Pavlichenko, Zh. Eksp. Teor. Fiz. **71**, 1755 (1976) [Sov. Phys. JETP **44**, 921 (1976)].
[3]L. Julien, M. Glass-Maujean, and J. P. Descoubes, J. Phys. B **6**, L196 (1976).
[4]G. F. Möhlmann, S. Tsurubuchi, and F. J. de Heer, Chem. Phys. **18**, 145 (1976).
[5]L. D. Weaver and R. H. Hughes, J. Chem. Phys. **52**, 2299 (1970).
[6]R. N. Zare and D. R. Herschbach, Proc. IEEE **51**, 173 (1963).
[7]R. N. Zare, J. Chem. Phys. **47**, 204 (1967).
[8]G. H. Dunn and L. J. Kieffer, Phys. Rev. **132**, 2109 (1963).
[9]R. J. Van Brunt and L. J. Kieffer, Phys. Rev. A **2**, 1293 (1970).
[10]D. A. Vroom and F. J. de Heer, J. Chem. Phys. **50**, 580 (1969).
[11]J. A. Schiavone, K. C. Smyth, and R. S. Freund, J. Chem. Phys. **63**, 1043 (1975).
[12]M. Misakian and J. C. Zorn, Phys. Rev. A **6**, 2180 (1972).
[13]P. Borrell, M. Glass-Maujean, and P. M. Guyon, Abstracts Fourth Intern. Conf. on Vacuum-Ultraviolet Radiat. Phys., Hamburg, 1974, p. 30.
[14]R. S. Berry and S. E. Nielson, Phys. Rev. A **1**, 395 (1970).
[15]A. L. Ford and K. K. Docken, J. Chem. Phys. **62**, 4955 (1975).
[16]R. S. Freund, J. Chem. Phys. **54**, 3125 (1971).
[17]K. C. Smith, J. A. Schiavone, and R. S. Freund, J. Chem. Phys. **59**, 5225 (1973).
[18]K. C. Smith, J. A. Schiavone, and R. S. Freund, J. Chem. Phys. **60**, 1358 (1974).
[19]C. Bottcher and K. Docken, J. Phys. B **7**, L5 (1974).
[20]C. Bottcher, J. Phys. B **7**, L352 (1974).
[21]A. U. Hazi, J. Phys. B **8**, L262 (1975).
[22]A. U. Hazi, J. Chem. Phys. **60**, 4358 (1974).
[23]A. U. Hazi, Chem. Phys. Lett. **25**, 259 (1974).



Translated by J. G. Adashko


# Technique of optical polarization measurements of plasma Langmuir turbulence spectrum


A. I. Zhuzhunashvili and E. A. Oks

*I. V. Kurchatov Atomic Energy Institute*



(Submitted 28 March 1977)
Zh. Eksp. Teor. Fiz. **73**, 2142–2156 (December 1977)



We describe an optical method of measuring the amplitude-angle distribution of a high-frequency Langmuir turbulence; the method is based on a polarization analysis of the Stark profiles of hydrogen spectral lines. We determine with the aid of this method, for the first time ever, both the turbulence level and the directivity pattern of the Langmuir noise produced in a plasma upon annihilation of opposing magnetic fields.



PACS numbers: 52.70.Kz, 52.35.Ra, 52.25.Ps


**1.** The development of spectroscopic diagnostics based on the Stark effect (see, e.g., [1]) has made possible a detailed investigation of the microscopic picture of the turbulent state of a plasma. The performance of such experiments has stimulated a successful development of the theory of Stark broadening of hydrogen and hydrogenlike lines by plasma noise. The theoretical procedure for measuring the level[2,3] and degree of anisotropy of the directivity pattern[4] of low-frequency (LF) noise was successfully put into effect in experiments[5,6]. In the theory of Stark broadening of hydrogen spectral lines by high-frequency (HF) Langmuir noise, the dominant role was played until recently by the adiabatic approximation.[7,8] The adiabatic theory, however, is not suitable for the calculation of the half-widths of lines having intense central components, such as $L_\alpha$, $H_\alpha$, $H_\gamma$, and others. For the remaining hydrogen lines, the adiabatic description of the noise action is suitable only under the following conditions: 1) the spectrum of the HF noise is one-dimensional; 2) the HF noise is polarized along the quasistatic field **F**; 3) the plasma has a one-dimensional quasistatic LF noise spectrum with average amplitude $F_0 \gg eN^{2/3}$ ($e$ is the electron charge and $N$ is the plasma concentration).[1)]

There have been a number of attempts to overcome the limitations in these calculations. Sholin[2] estimated the Stark-state lifetime determined by the nonadiabatic action of an HF noise spectrum of width $\Delta\Omega \sim \Omega_p$ ($\Omega_p$ is the plasma frequency). Kim and Wilhelm[9] calculated the analytic profile of the simplest hydrogen line $L_\alpha$ under the action of a three-dimensional HF noise spectrum but in the absence of a quasistatic electric field. In other theoretical papers, a computer was used to calculate the action of a static electric field crossed with an HF monochromatic electric field on the splitting



0038-5646/77/4606-1122$02.40

of the Lyman lines[10-12] and of the $H_\alpha$ line.[13]

For a long time, the authors of most spectroscopic investigations of hydrogen plasma with advanced Langmuir turbulence[14-17] attempted to interpret the results within the framework of the adiabatic theory.[7,8] One of the nonadiabatic effects of HF noise was revealed for the first time[18] in an experiment in which the increase of the half-width of the $H_\alpha$ line, predicted in[2], was observed. The authors of reports of later experiments[13,19,20] also understood the inconsistency of the adiabatic theory and the need for interpreting the registered profiles of the lines $H_\alpha$, $H_\beta$, $H_\gamma$, and $H_\delta$ with allowance for resonance between the HF and LF noise with mutually perpendicular polarizations. Computer calculations,[11,13] however, did not make it possible to extract reliable information from the experimental data, owing to the small number of the calculated line profiles and the limited character of the model, which did not take into account the finite width of the HF noise spectrum and the distribution of the magnitude of the (quasi)static field.

A consistent theory of the action of stochastic HF noise on a hydrogen atom with allowance for the simultaneous influence of quasistatic field was developed in[21]. It was shown there by analytic calculation that the joint action of the HF and LF components of the electric field causes not only the decrease predicted in[2] for the lifetime, but also a shift of the Stark states, and that both effects depend in resonant fashion on the intensity of the LF quasistatic field. In the resultant line profile there is not only a broadening of the central component, but also characteristic dips on the profile of the sideband components. These results have greatly improved the understanding of the experimental data of of[13,19,20]. However, the calculations in[21] were performed within the framework of perturbation theory and are valid only at relatively low amplitude of the HF noise.

We present here an additional analytic development of the theory proposed in[21] and go beyond the framework of perturbation theory; this enables us to extend substantially the region of validity of the theory and offer an incontrovertible interpretation of the experimental data of[13,19,20]. Results are presented of a spectroscopic investigation of the Langmuir turbulence in the "Dimpol" installation, in which, in particular, the polarization analysis proposed in[22] was carried out on the dips of the $H_\alpha$ line profile. The use of this procedure has made it possible to determine, for the first time, both the level and the directivity pattern of the Langmuir noise.

**2.** Under typical experimental conditions the average HF noise amplitude is $E_0 \ll |\mathbf{F}|$, so that the quasistatic field $\mathbf{F}$ determines the quantization of the hydrogen atom and splits the states with principal quantum number $n$ into $2n+1$ sublevels separated in frequency by $3nea_0F/2\hbar \equiv \omega_F$ ($a_0$ is the Bohr radius). When $\omega_F$ is close to the frequency $\omega_p$ of the HF noise, one can expect the appearance of nonadiabatic effects that deform the line profile.

The character of the response of the atom to stochastic HF noise depends essentially on the relation between the noise autocorelation time $\tau_c \sim \gamma_p^{-1}$ ($\gamma_p$ is the noise-spectrum half-width) and the characteristic time $\tau_m$ in which a substantial change takes place in the probability of finding the atom in a given Stark state. We have $\tau_m \sim \min(\tau_m^{ind}, \tau_m^{coll})$, where $\tau_m^{ind}$ and $\tau_m^{coll}$ characterize the action of the individual and collective components of the electric field of the plasma electrons. In the case when $\tau_c \ll \tau_m$ we can introduce the so-called "coarse-grain" time scale $\tau_c \ll \Delta t \ll \tau_m$. According to the theory of stochastic differential equations (see, e.g., [10]), at such time intervals $\Delta t$ the evolution of the state of the atom has the character of a Markov process and the solution is obtained within the framework of perturbation theory by expanding in the parameter $dE_0\tau_c/\hbar \ll 1$ ($\mathbf{d}$ is the operator of the dipole moment of the atom and $d$ is a characteristic value of its matrix elements). Calculation[21] has shown that in this case the action of the RF noise leads to the appearance of a width $\Gamma_\nu^{(p)}$ and a shift $D_\nu^{(p)}$ of the Stark state $\nu$, and these depend in resonant fashion on the quasistatic field (see formulas (10)–(12) of[21]; $\nu = \alpha$ corresponds to the initial Stark state and $\nu = \beta$ to the final one)[2)].

Thus, the time $\tau_m^{coll}$ is determined by the collective impact width $\Gamma_{\alpha\beta}^{(p)}$ of the $\alpha \to \beta$ Stark component calculated in[21], while the time $\tau_m^{ind}$ is determined by the electron impact width $\Gamma_{\alpha\beta}^{(e)}$, calculated in[23], of the same component. From the requirement $\tau_c \sim \gamma_p^{-1} \ll \tau_m \sim \min[(\Gamma_{\alpha\beta}^{(e)})^{-1}, (\Gamma_{\alpha\beta}^{(e)})^{-1}]$ it follows that introduction of the "coarse-grain" time scale is possible if the following conditions are satisfied:

$$\gamma_p \gg \Gamma_\nu^{(e)} \quad (\nu=\alpha,\beta), \qquad \varepsilon_\nu^2 = \frac{3n_\nu^2[n^2-(n_1-n_2)^2-m^2-1]_\nu e^2a_0^2E_0^2}{32\hbar^2} \ll [\gamma_p^2+(\omega_F-\Omega_p)^2] \ll \Omega_p, \tag{1}$$

where $n_1$, $n_2$, and $m$ are parabolic quantum numbers. In the opposite limiting case $\gamma_p \ll \Gamma_{\alpha\beta}^{(e)}$, introduction of the "coarse-grain" time scale is not justified, because $\tau_m \lesssim (\Gamma_{\alpha\beta}^{(e)})^{-1} \ll \tau_c \sim \gamma_p^{-1}$, so that over times $\Delta\tau \sim \tau_m$ the stochastic character of the action of the HF noise does not manifest itself.

**3.** In the case when the amplitude of the HF noise $E_0$ is large enough, so that

$$\varepsilon_\nu \gg \max(\gamma_p, |\omega_F-\Omega_p|, \Gamma_{\alpha\beta}^{(e)}) \quad (\nu=\alpha,\beta) \tag{2}$$

(but $E_0 \ll F$ as before), the perturbation-theory calculations used in[21] do not hold for any ratio of $\gamma_p$ and $\Gamma_\alpha^{(e)}$, since the expansion parameter $[\varepsilon_\nu/\max(\gamma_p, |\omega_F-\Omega_p|, \Gamma_{\alpha\beta}^{(e)})]^2 \gg 1$. In this case it is possible to obtain an exact solution for the evolution operator in the resonance region: $|\omega_F - \Omega_p| \ll \varepsilon_\nu$.[3)]

We consider first the simplest particular case of transitions induced by HF noise between Stark sublevels within the principal quantum number $n=2$. We relabel these Stark states as follows: $(100) = +1$; $(010) = -1$; $(00+1) = +0$; $(00-1) = -0$. The known quantum-mechanical equations for the matrix elements of the evolution operator $T(\tau)$ of an atom in an electric field are of the form

$$i\hbar\dot{T}_{\alpha\alpha''}=\sum_{\alpha'}\exp\{i\omega_{\alpha\alpha'}\tau\}\mathbf{d}_{\alpha\alpha'}\mathbf{E}(\tau)\cos(\Omega_p\tau+\varphi(\tau))T_{\alpha\alpha''};$$
$$|T_{\alpha\alpha''}(0)|=\delta_{\alpha\alpha''}. \tag{3}$$

The time dependences of the phase and amplitude of the electric field of the HF noise can be disregarded, since it will be shown that only time intervals $\Delta\tau\ll\tau_c\sim\gamma_p^{-1}$ are significant in the long run. In the resonance approximation we get from (3) the following system of equations (we put $q=\omega_F-\Omega_p$):

$$\begin{aligned}
i\hbar\dot{T}_{\pm0\pm0}&=\tfrac{1}{2}\mathbf{E}[\mathbf{d}_{\pm0-1}e^{iq\tau-i\varphi}T_{-1\pm0}+\mathbf{d}_{\pm0+1}e^{-iq\tau+i\varphi}T_{+1\pm0}],\\
i\hbar\dot{T}_{-0+0}&=\tfrac{1}{2}\mathbf{E}[\mathbf{d}_{-0-1}e^{iq\tau-i\varphi}T_{-1+0}+\mathbf{d}_{-0+1}e^{-iq\tau+i\varphi}T_{+1+0}],\\
i\hbar\dot{T}_{\pm1\pm1}&=\tfrac{1}{2}\mathbf{E}[\mathbf{d}_{\pm1+0}e^{\pm iq\tau\mp i\varphi}T_{+0\pm1}+\mathbf{d}_{-0+1}e^{\pm iq\tau\mp i\varphi}T_{-0\pm1}],\\
i\hbar\dot{T}_{+1\pm0}&=\tfrac{1}{2}e^{iq\tau-i\varphi}\mathbf{E}(\mathbf{d}_{+1+0}T_{+0\pm0}+\mathbf{d}_{+1-0}T_{-0\pm0}),\\
i\hbar\dot{T}_{-1\pm0}&=\tfrac{1}{2}e^{-iq\tau+i\varphi}\mathbf{E}(\mathbf{d}_{+1-0}T_{+0\pm0}+\mathbf{d}_{-1-0}T_{-0\pm0}),\\
i\hbar\dot{T}_{-1+1}&=\tfrac{1}{2}e^{-iq\tau-i\varphi}\mathbf{E}(\mathbf{d}_{-1\pm0}T_{+0+1}+\mathbf{d}_{-1-0}T_{-0+1}).
\end{aligned}$$

Each of these formulas contains two equations corresponding to the upper or lower sign of the state index. The ten equations written here suffice to determine all sixteen matrix elements $T_{\alpha\alpha'}$, since $T_{\alpha\alpha'}=T^*_{\alpha'\alpha}$.

At exact resonance $\Omega_p=\omega_F$ the solutions of the system, averaged over the random phase of the HF noise, are of the form

$$-T^{(I)}_{+1+1}=T^{(I)}_{+0+0}=T^{(I)}_{-0-0}=-T^{(I)}_{-1-1}=\cos\varepsilon\tau,$$
$$T^{(II)}_{+0+0}=-T^{(II)}_{-0-0}=\cos\varepsilon\tau,\quad T^{(II)}_{+1+1}=-T^{(II)}_{-1-1}=e^{i\psi}$$

($\psi$ is some real number; the off-diagonal matrix elements in both solutions are equal to zero).

The results signify that at resonance $\Omega_p=\omega_F$ the probability of finding an atom on a Stark sublevel $\alpha$ oscillates with frequency $2\varepsilon_\alpha$. These oscillations of the solutions obtained in the resonance approximation are not unexpected. Similar oscillations of the populations of a two-level system resonantly acted upon by a monochromatic field with a fixed phase are described, for example, in[26,27] and in the books[28,29]. At inexact resonance the oscillation frequency is

$$2\varepsilon_\alpha=[(2\varepsilon_\alpha)^2+(\omega_F-\Omega_p)^2]^{1/2}. \tag{4}$$

This formula is valid only at $|\omega_F-\Omega|\ll\varepsilon_\alpha$, so that in fact there is no need to take the detuning into account. The evolution of the state has an essentially non-Markov character. The characteristic evolution time is $\tau_m\sim\varepsilon_\alpha^{-1}\ll\tau_c\sim\gamma_p^{-1}$, so that the approximation made on going from formula (3) to the system of equations written out above is justified.

Although the results were obtained for the simplest case $n=2$, they are of more general character. This is due first, to the fact that within the set of $n^2$ Stark states $(n_1n_2m)$ with principal quantum number $n$, each of them is coupled by a dipole transition only with the two neighboring states with $n'=m\pm1$; and second, to the averaging over the phases of the HF noise. Therefore in the system of $n^2(n^2+1)/2$ equations that connect the quantities $T_{\alpha\alpha'}$, any group of equations of the type[4)]

$$i\hbar\dot{T}_{\alpha\alpha}=\tfrac{1}{2}\mathbf{E}(\mathbf{d}_{\alpha\alpha-1}T_{\alpha-1\alpha}e^{-i\varphi}+\mathbf{d}_{\alpha\alpha+1}T_{\alpha+1\alpha}e^{+i\varphi}), \tag{5}$$
$$i\hbar\dot{T}_{\alpha-1\alpha}=\tfrac{1}{2}\mathbf{E}(\mathbf{d}_{\alpha-1\alpha}T_{\alpha\alpha}e^{+i\varphi}+\mathbf{d}_{\alpha-1\alpha-1}T_{\alpha-1\alpha}e^{-i\varphi}), \tag{6}$$
$$i\hbar\dot{T}_{\alpha+1\alpha}=\tfrac{1}{2}\mathbf{E}(\mathbf{d}_{\alpha+1\alpha}T_{\alpha\alpha}e^{-i\varphi}+\mathbf{d}_{\alpha+1\alpha+1}T_{\alpha+2\alpha}e^{+i\varphi}), \tag{7}$$

forms a relatively independent block. Substituting (6) and (7) in the differentiated equation (5), we get

$$-\hbar^2\ddot{T}_{\alpha\alpha}=[(\tfrac{1}{2}\mathbf{E}\mathbf{d}_{\alpha\alpha-1})(\tfrac{1}{2}\mathbf{E}\mathbf{d}_{\alpha-1\alpha})+(\tfrac{1}{2}\mathbf{E}\mathbf{d}_{\alpha\alpha+1})(\tfrac{1}{2}\mathbf{E}\mathbf{d}_{\alpha+1\alpha})]T_{\alpha\alpha},$$

whence we get for $T_{\alpha\alpha}\equiv T^{n_1n_2m}_{n_1'n_2'm}$ a solution that oscillates with a frequency

$$\begin{aligned}
\varepsilon_{n_1n_2m}&=\frac{E_0}{\hbar\sqrt{12}}[|\mathbf{d}^{n_1n_2m}_{n_1'n_2'm-1}|^2+|\mathbf{d}^{n_1n_2m}_{n_1''n_2''m+1}|^2]^{1/2}\\
&=\frac{6^{1/2}ea_0E_0}{8\pi}[n^2-(n_1-n_2)^2-m^2-1]^{1/2}.
\end{aligned} \tag{8}$$

When the condition (2) is satisfied, and in particular the condition of the resonance of the plasma frequency with the splitting of the upper or lower of the multiplets making up the spectral line,

$$|\Omega_p-\omega_F^{(\nu)}|\ll\varepsilon_\nu\quad\left(\omega_F^{(\nu)}=\frac{3ea_0F}{2\hbar}n_\nu,\ \nu=\alpha,\beta\right),$$

the Stark component $S_{\alpha\beta}(\omega,F)$ is split into two dispersion contours of equal intensity, separated from each other in frequency by $2\varepsilon_\nu$. These contours are characterized by a half-width $\Gamma^{(e)}_{\alpha\beta}+\gamma_p$ and by an additional shift $D^{(e)}_{\alpha\beta}$.

**4.** The total profile of the Stark component $S_{\alpha\beta}(\omega)$ is obtained by averaging the profile of the subline $S_{\alpha\beta}(\omega,F)$ over the distribution of the quasistatic fields $W_{st}(F)dF$:

$$S_{\alpha\beta}(\omega)=\int_0^\infty dF\,W_{st}(F)S_{\alpha\beta}(\omega,F).$$

The formulas obtained in[21] for $S_{\alpha\beta}(\omega,F)$ are valid for all $F$ only in the case when $\varepsilon_\nu\lesssim\gamma_p$. On the other hand, in the case of large HF noise amplitudes, when $\varepsilon_\nu\gg\gamma_p$, the region of integration with respect to $F$ breaks up, in general, into five parts: on the intervals

$$L_\alpha(\Omega_p-\varepsilon_\alpha)<F<L_\alpha(\Omega_p+\varepsilon_\alpha),\quad L_\beta(\Omega_p-\varepsilon_\beta)<F<L_\beta(\Omega_p+\varepsilon_\beta)$$
$$(L_\nu=2\hbar/3ea_0n_\nu)$$

it is necessary to use in lieu of the subline $S_{\alpha\beta}(\omega,F)$ profile calculated in[21] the split contour described in Sec. 3 of the present paper. This calculation shows that the following singularities arise on the Stark profiles of hydrogen spectral lines under the influence of the HF noise:

*Central component.* The increase of the half-width is

$$\Delta\omega_{1/2}^{(p)}=2\gamma_p(\varepsilon_\alpha^2+\varepsilon_\beta^2)/\Omega_p^2,\quad \max(\omega_{F_0}^{(\alpha)},\omega_{F_0}^{(\beta)})\ll\Omega_p.$$
$$\Delta\omega_{1/2}^{(p)}=2\gamma_p[(\varepsilon_\alpha/\omega_{F_0}^{(\alpha)})^2+(\varepsilon_\beta/\omega_{F_0}^{(\beta)})^2],\quad \min(\omega_{F_0}^{(\alpha)},\omega_{F_0}^{(\beta)})\gg\Omega_p.$$

*Sideband component.* Dips appear on its contour at the following frequencies:

$$\begin{aligned}
\omega_\alpha&=\left[(n_1-n_2)_\alpha-\frac{n_\beta}{n_\alpha}(n_1-n_2)_\beta\right]\Omega_p,\\
\omega_\beta&=\left[\frac{n_\alpha}{n_\beta}(n_1-n_2)_\alpha-(n_1-n_2)_\beta\right]\Omega_p.
\end{aligned} \tag{9}$$

In the wavelength scale this corresponds to distances $\lambda_\alpha$ and $\lambda_\beta$ from the center of the line $\lambda_0$, defined as

$$\lambda_\alpha=\omega_\alpha\lambda_p/\Omega_p,\quad \lambda_\beta=\omega_\beta\lambda_p/\Omega_p,\quad \lambda_p=\Omega_p\lambda_0^2/2\pi c. \tag{9'}$$

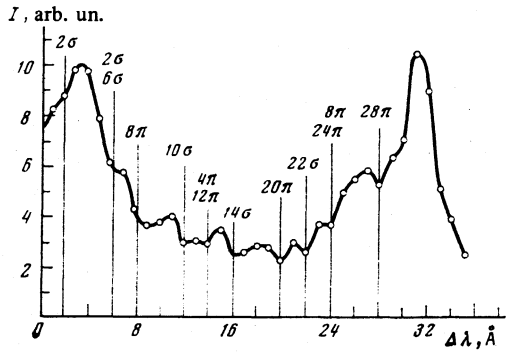


FIG. 1. Experimental profile of the spectral line $H_\delta$ from[19]. The strokes mark the dip positions expected in accord with the results of the theory of nonadiabatic action of the RF noise on the hydrogen atom. The Stark components pertaining to particular dips are indicated. The upper and lower rows of indices indicate dips produced as a result of resonance between the frequency of the RF noise and the static splitting of the multiplet with $n_\alpha = 6$ and $n_\beta = 2$.

In the case of a large HF noise amplitude, when $\varepsilon_\nu \gg (\gamma_p + \Gamma_{\alpha\beta}^{(e)})$ (but $E_0 \ll F_0$), the dips are most strongly pronounced, and the half-width of the dip is equal to

$$\Delta\omega_{1/2}^{gap} = \omega_\nu \varepsilon_\nu / \Omega_p, \quad \nu = \alpha, \beta, \tag{10}$$

i.e., it is proportional to the amplitude $E_0$ of the HF noise.

Thus, the singularities of the profile of the hydrogen spectral line at the frequencies $\omega \sim \Omega_p$ are practically always due to nonadiabatic action of the Langmuir noise. The experimentally measured half-width $\Delta\lambda_{1/2}^{gap}$ of the dip makes it possible to determine the average amplitude $E_0$ of the Langmuir noise. In fact, from (8)–(10) we get

$$E_0[\text{kV/cm}] = \frac{7.6\cdot 10^8 [\Delta\lambda_{1/2}^{gap}, \text{Å}]}{[n_\nu^2 - (n_1 - n_2)_\nu^2 - m_\nu^2 - 1]^{1/4} |n_\alpha (n_1 - n_2)_\alpha - n_\beta (n_1 - n_2)_\beta| [\lambda_0, \text{Å}]} \tag{11}$$

$(\nu = \alpha, \beta)$.

The validity of the interpretation based on the non-

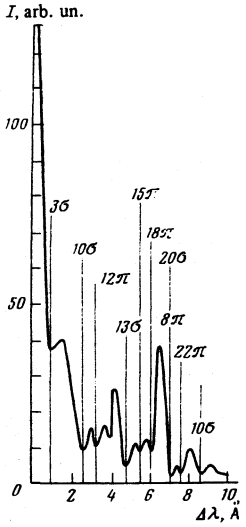


FIG. 2. Experimental profile of $H_\gamma$ line from[13]. The dip positions theoretically expected as a result of resonance between $\omega_{HF}$ and the splitting of the multiplet in static fields $F_0$ with $n_\alpha = 5$ and $n_\beta = 2$ are marked.

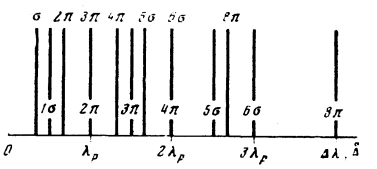


FIG. 3. Positions of dips produced on the profile of the line $H_\alpha$ on account of resonance between $\omega_{HF}$ and the splitting of the multiplet in static fields with $n_\alpha = 3$ and $n_\beta = 2$.

adiabatic theory can be confirmed by examining the profiles of the $H_\delta$ and $H_\gamma$ lines measured in[19,13]. Figure 1 shows the experimental profile of $H_\delta$ from[19], with marked positions of the dips expected in accordance with the results of[21,24] described above. The reference point was the position of the dip at the distance $\lambda \approx 28$ Å from the line center, identified with the position of one of two dips (the nearest to the center) on the profile of the most intense $28\pi$ component. Figure 2 shows the experimental profile of $H_\gamma$ from[13], on which the theoretically expected positions of the dips are also marked. It is seen that all the indicated dip positions agree well with those measured in experiment.

The agreement between the developed theory and experiment is most clearly manifest on hydrogen lines with a large number of Stark components and hence a large number of dips ($H_\gamma$, $H_\delta$, and others). On a line with few dips, however, it is possible to measure with greater accuracy the dip half-width and determine from (11) the HF noise intensity. It is therefore advantageous to use from the Balmer series the $H_\alpha$ line. The expected positions of the dips on the $H_\alpha$ profile are indicated in Fig. 3.

**5.** Nonadiabatic effects are maximal at mutually perpendicular orientations of the LF and HF fields $\mathbf{F} \perp \mathbf{E}$ and are completely lacking at $\mathbf{F} \parallel \mathbf{E}$. This enables us to apply a polarization analysis for the investigation of the HF noise anisotropy. In the case when the HF noise distribution has a symmetry axis, it is best to carry out the polarization analysis by extracting light from the system in a direction perpendicular to this axis. Then the polarizer transmission axis can be oriented in positions 1 and 2: parallel and perpendicular to the symmetry axis, respectively. In[22] it was proposed to use as the experimentally measured quantity the relative change of the dip half-width at two positions of the polarizer transmission axis:

$$1.5\frac{(\Delta\lambda_{1/2}^{gap})_{1\chi} - (\Delta\lambda_{1/2}^{gap})_{2\chi}}{0.5(\Delta\lambda_{1/2}^{gap})_{1\chi} + (\Delta\lambda_{1/2}^{gap})_{2\chi}} \equiv P_\chi(\mu), \tag{12}$$

where $\mu \equiv [\langle E_1^2\rangle / \langle E_2^2\rangle]^{1/2}$ is the degree of anisotropy of the HF noise; the index $\chi = \pi, \sigma$ corresponds to polarization of the Stark component on whose profile the dip is observed. It turns out that the quantities $P_\chi(\mu)$ for $\pi$ and $\sigma$ dips are connected by the relation $P_\chi(\mu) = -2P_\sigma(\mu)$. The calculated dependence of $P_\sigma$ on $\mu$ for isotropic distribution of the LF quasistatic fields is shown in Fig. 4.

**6.** The experiments were performed with "Dimpol" installation. In our preceding study,[5] in which we determined the directivity pattern of the LF noise of a

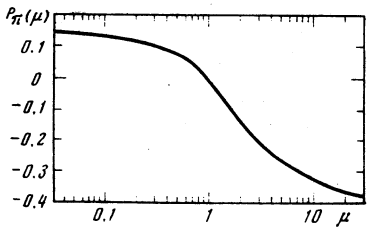


FIG. 4. Calculated dependence of the relative change of the dip half-width at two mutual perpendicular of the polarizer axis, $P_\pi(\mu)$, on the degree of anisotropy $\mu = (\langle E_1^2\rangle / \langle E_2^2\rangle)^{1/2}$.

plasma, we described in detail the setup, the measurement apparatus, and the measurement procedure. In the present paper we present results of further experiments on the "Dimpol" setup, in which we investigated in detail the Langmuir turbulence. Most experiments were performed on hydrogen, since its spectral lines provide, in accord with the theory described above, the most exact information on the RF noise of the plasma. Nonetheless, some of the experiments were performed on helium, so as to demonstrate one more method of LF noise diagnostics.

Figure 5 shows the profiles of the interference orders of the lines HeI 4471.48 Å (allowed transition $2^3P$–$4^3D$) and 4469.92 Å (forbidden transition $2^3P$–$4^3F$), obtained by reducing the spectrochronogram with an IFO-451 microphotometer. The profiles were registered by observation in a transverse direction without a polarizer. The allowed line is shown in the second interference order, a fact indicated on the figure by the symbol II A; the forbidden line is shown in first and second interference orders (I F and II F). The distance between the orders (the dispersion region) is 3.34 Å. The experimentally measured distance between the allowed (II A) and forbidden (II F) lines is $\Delta\lambda \approx 2$ Å. In the absence of electric fields this distance, as is well known, is $\Delta\lambda_0 = 1.56$ Å. Since the states $4^3D$ and $4^3F$ can be regarded with sufficient accuracy as a two-level system, it follows that the dependence of $\Delta\lambda$ on the (quasi) static electric field $F$ is of the form

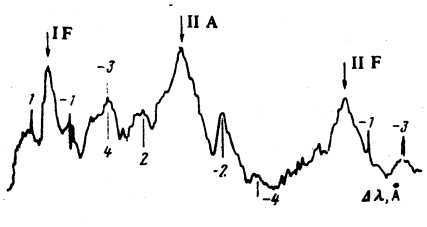


FIG. 5. Profiles of interference order of the spectral lines He I 4471.48 Å (allowed transition $2^3P-4^3D$) and 4469.92 Å (forbidden transition $2^3P-4^3F$) in transverse observation. The distance between the allowed interference orders in 3.34 Å. The allowed line is shown in second interference order (II A), and the forbidden one in first and second interference orders (I F, II F). The locations of the satellites relative to the allowed and forbidden lines are indicated by vertical straight-line segments. The satellite shift is indicated above the segment if it is relative to a forbidden line and under the segment in the case of an allowed line.

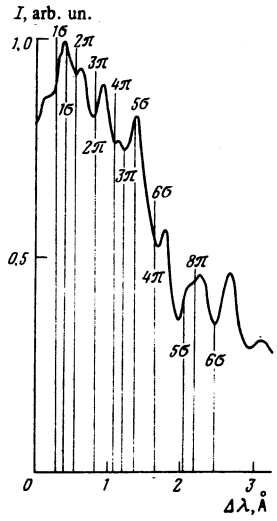


FIG. 6. Profile of registered $H_\alpha$ in longitudinal observation without a polarizer. The vertical segments indicate the theoretically expected dip positions.

$$\Delta\lambda = \left[ (\Delta\lambda_0)^2 + \left(\frac{\lambda_0^2}{2\pi c}\right)^2 \frac{4F^2}{\hbar^2} \sum_{m'} |\langle l_m | \mathbf{d} | l_{m'}' \rangle|^2 \right]^{1/2}$$

$$= \left[ (\Delta\lambda_0)^2 + \left(\frac{\lambda_0^2}{2\pi c}\right)^2 \frac{4e^2 a_0^2 R_{ll'} F^2}{\hbar^2} \right]^{1/2}, \qquad (13)$$

where $\lambda_0 = \frac{1}{2}(\lambda_1 + \lambda_2) = 4470.70$ Å is the average wavelength; the dimensionless quantities $R_{ll'}$ for the different pairs of helium lines are given in[30,1]. In particular, for the states $4^3D$ and $4^3F$ we have $R_{ll'} = 1.51$ and by substituting the numerical values in (13) we get $F = 6$ kV/cm.

The calculated intensity of the LF quasistatic fields is less than the value 31 kV/cm measured earlier for a hydrogen plasma. The reason is that the experiment on helium was carried out at a lower amplitude of the alternating magnetic field $\bar{H}$ than for hydrogen. If $\bar{H}$ were not decreased, the high intensity of the LF fields, $F \gg \pi mce\Delta\lambda_0/(R_{ll'})^{1/2}\hbar\lambda_0^2 \approx 7$, would lead, according to (13), to a transition to the regime of the linear Stark effect, in which there is no longer any fundamental difference between the helium and hydrogen spectral lines.

The obtained profiles show clearly satellites whose positions are marked by vertical line segments. The satellite shift, in units of $\lambda_p \equiv \Omega_p \lambda_0^2/2\pi c$, relative to the forbidden line is indicated above the segment, and relative to the allowed line below the segment.[5)] The satellite positions form the regular pattern predicted in[27,28,30,31]. The experimentally measured value $\lambda_p \approx 0.23$ Å makes it possible to determine the plasma concentration $N = \pi mc^2\lambda_p^2/e^2\lambda_0^4 \approx 1.4\times10^{13}$ cm$^{-3}$. We note that the individual LF-field component $F_{ind} \approx 2.6\, eN^{2/3} \approx 0.2$ kV/cm is only a small fraction of the measured LF field $F \approx 6$ kV/cm, which consequently agrees with good accuracy with the LF noise field.

Thus, the appearance of forbidden helium lines can be used to measure LF-noise field intensities, using formula (13). As to the determination of the HF noise amplitude $E_0$, this calls according to[30,31] for measurement of the relative area under the satellites. First, however, it is seen from the experimental profiles on Fig. 6 that the accuracy of such a measurement is low.

Second, it follows from the theory[30,31] that the measured quantity is proportional to $E_0^2$ even for the satellite closest to the forbidden line, whereas on hydrogen it is possible to measure a quantity (the dip half-width) proportional to $E_0$, thus greatly increasing the accuracy with which $E_0$ is determined. Therefore the measurement of the amplitude-angle distribution of the Langmuir noise was carried out on hydrogen.

7. The experiments on hydrogen were performed in the same regime as the previous ones.[5] Figure 6 shows the profile of the $H_\alpha$ line, registered in longitudinal observation without a polarizer. The vertical line segments indicated the theoretically expected dip positions (cf. Fig. 3). It is seen that the measured decreases of the profiles coincide exactly with the positions of nine (out of 12 expected) dips and correspond to the distances $\lambda_p/3=\lambda_{101}^{1\sigma}$, $2\lambda_p/3=\lambda_{110}^{2\pi}$, $\lambda_p=\lambda_{101}^{3\pi}=\lambda_{010}^{2\pi}$, $4\lambda_p/3=\lambda_{200}^{4\pi}$, $3\lambda_p/2=\lambda_{001}^{3\pi}$, $2\lambda_p=\lambda_{100}^{4\pi}=\lambda_{200}^{6\sigma}$, $5\lambda_p/2=\lambda_{010}^{5\sigma}$, $8\lambda_p/3=\lambda_{200}^{8\pi}$, $3\lambda_p=\lambda_{001}^{6\sigma}$. The three remaining dips could appear at the distances $\lambda_p/2=\lambda_{100}^{1\sigma}$, $5\lambda_p/3=\lambda_{101}^{5\sigma}$, $4\lambda_p=\lambda_{010}^{8\pi}$. The dips at the distances $\lambda_p/2$ and $5\lambda_p/3$ have apparently merged with the dips at the respective distances $2\lambda_p/3$ and $3\lambda_p/2$; the distance $4\lambda_p$ at which the last dip was expected corresponds to a remote wing outside the measured band. The value $\lambda_p\approx 0.87$ Å measured in accord with the indicated structure makes it possible to determine the plasma concentration, namely $N\approx 4.5\times10^{13}$ cm$^{-3}$.

Instead of the dip half-width, it is more convenient to measure its equivalent, the distance between the center of the dip and the nearest "hill." This measurement can be carried out with sufficient accuracy on six dips of the $H_\alpha$ profile shown in Fig. 6: $(\Delta\lambda)_{2/3}\approx 0.11$ Å, $(\Delta\lambda)_1\approx 0.15$ Å, $(\Delta\lambda)_{3/2}\approx 0.11$ Å, $(\Delta\lambda)_2\approx 0.14$ Å, $(\Delta\lambda)_{5/2}\approx 0.16$ Å, $(\Delta\lambda)_3\approx 0.22$ Å (the subscript of $\Delta\lambda$ indicates the distance from the dip to the line center in units of $\lambda_p$). Substituting the measured half-widths in (11), we obtain for the average HF noise amplitude $E_0=4.3\pm0.5$ kV/cm. Since the previously measured[5] rms LF noise intensity is $F_0\approx 31$ kV/cm, the necessary condition for the applicability of the proposed procedure, $E_0\ll F_0$, is satisfied.

To determine the directivity pattern of the Langmuir noise we introduced in the optical system a polaroid polarizer, which made it possible, in transverse observation, to separate the $z$ and $\varphi$ polarization, and in longitudinal observation the $r$ and $\varphi$ polarizations (the unit vectors of the cylindrical coordinate system are indicated in Fig. 7). Figure 8 shows typical $z$- and

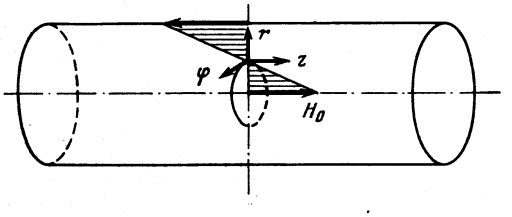


FIG. 7. Unit vectors of cylindrical coordinate system used to analyze the distributions of the LF and HF turbulent fields in the plasma.

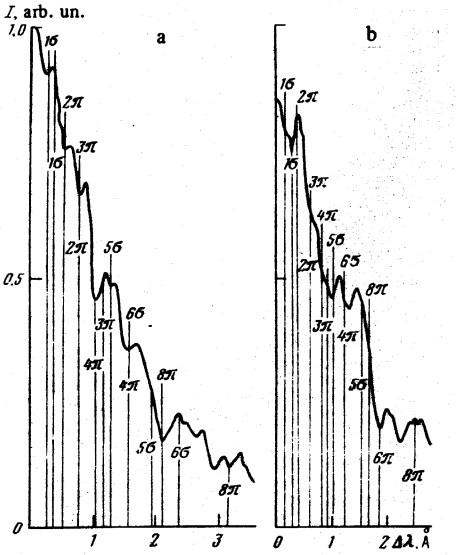


FIG. 8. Polarization contours of interference order of the $H_\alpha$ line, obtained with polarizer axis oriented in the plane $z$ (a) and $\varphi$ (b) in transverse observation.

$\varphi$-polarization contours obtained in transverse observation, while Fig. 9 shows $r$- and $\varphi$-polarization contours obtained in longitudinal observation. The value of $\lambda_p$ determined by measuring the distance between the dips is the same for all four contours and amounts to $\lambda_p\approx 0.76$ Å, which corresponds to a plasma concentration $N\approx 3.4\times10^{13}$ cm$^{-3}$. The slight decrease of the concentration from the previously measured $N\approx 4.5\times10^{13}$ cm$^{-3}$, obtained by a certain decrease of the hydrogen pressure, was produced to make the dip farthest from the $8\pi$ component in the line wing fall in the measured band 3.6 Å.

When comparing the corresponding dips on the polarization profiles, it must be taken into account that according to the nonadibatic theory the dip should be flanked by two "hills," which compensate for the nor-

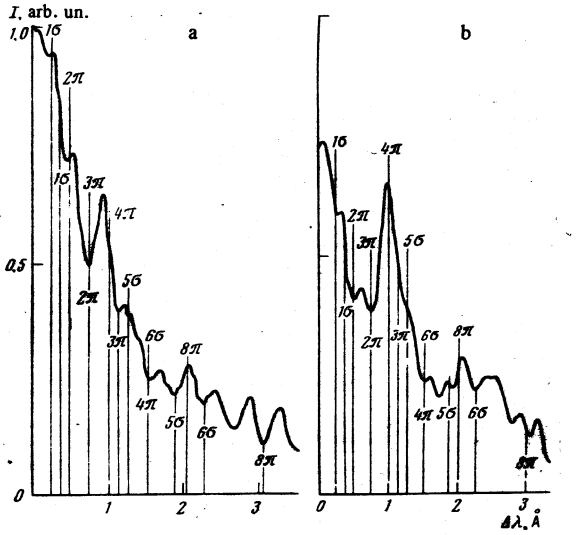


FIG. 9. Polarization contours of interference order of $H_\alpha$ line obtained with the polarizer electric axis in the planes $r$ (a) and $\varphi$ (b) in longitudinal observation.

malization. However, a close proximity of two dips leads as a rule to observation of only one hill between them, rather than two. Thus, close proximity of two or more dips distorts the results of the measurement of their half-widths. This effect can exceed the polarization difference between the half-width of the dip on the $r$ and $\varphi$ profiles. Therefore the most reliable results are obtained from a polarization analysis of well isolated dips. On the $H_\alpha$ profile, the most isolated of all the dips is at the distance $4\lambda_p = \lambda_{010}^{8\pi}$. Between this dip and the nearest dip of wavelength $\lambda_{001}^{6\sigma} = 3\lambda_p$ are observed two "hills" on each of the polarization profiles (Figs. 8 and 9). To some degree, the dips at the distances $\lambda_p$, $2\lambda_p$, and $3\lambda_p$ can also be regarded as isolated. A statistical comparison of the half-widths of these dips on the $z$ and $\varphi$ profiles, carried out for different profile pairs obtained in transverse observation revealed no noticeable polarization difference between the half-widths: $(\Delta\lambda_{1/2}^{exp})_{\pi\pi} \approx (\Delta\lambda_{1/2}^{exp})_{\varphi\varphi}$, $(\Delta\lambda_{1/2}^{exp})_{\pi\sigma} \approx (\Delta\lambda_{1/2}^{exp})_{\varphi\sigma}$, and consequently $(\langle E_\pi^2\rangle) \approx (\langle E_\varphi^2\rangle)$. A comparison of the half-widths of the same dips on the $r$ and $\varphi$ profiles obtained in longitudinal observation shows that $(\Delta\lambda_{1/2}^{exp})_{r\pi} > (\Delta\lambda_{1/2}^{exp})_{\varphi\pi}$, $(\Delta\lambda_{1/2}^{exp})_{r\sigma} < (\Delta\lambda_{1/2}^{exp})_{\varphi\sigma}$. In accordance with the theoretical results given in Sec. 5 of the present paper, this means that $(\langle E_r^2\rangle) < (\langle E_\varphi^2\rangle)$. Thus, the directivity pattern of the Langmuir noise takes the form of an oblate ellipsoid of revolution with axis along $r$.

The presence of a symmetry axis allows us to use, for a quantitative analysis, the function $P_\pi(\mu) = -2P_\sigma(\mu) \equiv P(\mu)$ shown in Fig. 4. By calculating with the aid of (12) the experimental values $P_\pi$ and $(-2P_\sigma)$ for the corresponding dips on the $r$ and $\varphi$ profiles and averaging the values obtained for different dips and different pairs of polarization profiles, we get $P(\mu) = 0.12 \pm 0.06$. The plot shown in Fig. 4 allows us to draw the following conclusion: the degree of anisotropy is $\mu \equiv [\langle E_r^2\rangle / \langle E_\varphi^2\rangle]^{1/2} < 0.5$, and the most probable value is $\mu \approx 0.1$.[6)]

Thus, the directivity pattern of the Langmuir noise is characterized by the following quantities: $\sqrt{\langle E_\varphi^2\rangle} \approx \sqrt{\langle E_\varphi^2\rangle} \approx 3$ kV/cm and $\sqrt{\langle E_r^2\rangle} \approx 0.3$ kV/cm.

8. It was shown in the present paper that the spectroscopic procedure based on the nonadiabatic theory of the Stark broadening of hydrogen lines by HF plasma noise makes it possible to measure the amplitude and degree of anisotropy of the Langmuir noise. The sensitivity and accuracy of this procedure is substantially higher than that of the diagnostic method based on the appearance of satellites of forbidden helium lines.

The most complete information on Langmuir noise can can be extracted from the profile of the hydrogen line in the case when the half-width of the dips exceeds the characteristic scales of the electron impact broadening $\Delta\lambda_e \sim (\Gamma^{(e)} + \Gamma^{(p)})\lambda_0^2/2\pi c$ and the Doppler broadening $\Delta\lambda_D \sim \lambda_0\sqrt{T_a/Mc^2}$ ($T_a$ is the atom temperature and $M$ is their mass). Under typical experimental conditions we have $\Delta\lambda_D > \Delta\lambda_e$. The quantity $\Delta\lambda_{1/2}^{exp}$, as follows from (11), is linear in the HF noise amplitude $E_0$, for which we have a lower bound

$$E_0 < F_0 \leqslant \sqrt{8\pi N T_e}. \qquad (14)$$

From the condition $\Delta\lambda_{1/2}^{exp} > \Delta\lambda_D$, by using formulas (11) and (14), we can obtain the concentration and temperature regions of applicability of the procedure. For the $H_\alpha$ line, in particular, we have

$$N(\text{cm}^{-3}) \gg 6 \cdot 10^{11} T_a/T_e. \qquad (15)$$

If this condition is not satisfied, then it is more reasonable to change over in the experiment to higher members of the Balmer series where $\Delta\lambda_{1/2}^{exp} > \Delta\lambda_D$ ($\Delta\lambda_{1/2}^{exp} \propto n^3$, and $\Delta\lambda_D$ decreases with increasing $n$).

Under the conditions of the present experiment, $N = 3.4 \times 10^{13}$ cm$^{-3}$ and $T_e \sim 10^3$ eV, and the atom temperature determined by measuring the Doppler broadening of the central part of the $H_\alpha$ line is $T_a = 50$–$90$ eV, so that the condition (15) is satisfied. The measured amplitude of the Langmuir noise corresponds to a turbulence level $E_0^2/8\pi n T_e \sim 10^{-4}$, which greatly exceeds the thermal level. Indeed, in a two-temperature plasma that is in a partial thermodynamic equilibrium, the noise amplitude $E_{0T}$ is

$$E_{0T} = (4\pi N_e^2)^{1/4}(T_e + T_i)^{1/4}/(T_e T_i)^{1/4}.$$

Substituting $N = 3.4 \times 10^{13}$ cm$^{-3}$ and $T_e \approx 10^3$ eV, and assuming $T_e/T_i = 10$–$40$, we get $E_{0T} = 0.2$–$0.4$ kV/cm, which is much less than the measured $E_0 = 4.3 \pm 0.5$ kV/cm.

The calculated value of $E_{0T}$ agrees with the measured value $\sqrt{\langle E_r^2\rangle} \approx 0.3$ kV/cm.

Upon annihilation of opposing magnetic fields on the surface, corresponding to a zero magnetic field, a plasma layer is produced with a maximal concentration. It was established in the present paper that not only LF instabilities but also Langmuir noises develop in this layer. Since clearly pronounced dips were registered on the $H_\alpha$ line profiles, it appears that the Langmuir turbulence is effectively developed within the limits of the layer in which the plasma concentration varies insignificantly. Indeed, it follows from (9) that the positions of the dips are $\lambda_{\alpha_s\beta} \sim N^{1/2}$, so that substantial plasma inhomogeneities would cause a "smearing" and in fact a vanishing of the dips. The polarization analysis shows that the Langmuir-noise fields are oriented in the "current–magnetic field" plane, which is tangent to the plasma layer. Therefore, although an unambiguous interpretation of the established form of the directivity pattern on the basis of the available data is difficult, one can nevertheless assume that in a plasma layer of thickness $\delta$ there develops a fundamental Langmuir mode having, in particular, a radial wave vector component $k_r \sim \delta^{-1}$.[7)]

The authors are deeply grateful to Professor L. I. Rudakov for a useful discussion and valuable advice.

[1)] If an individual quasistatic field component due to the random thermal motion of the individual particles predominates over the collective component ($eN^{2/3} \gg F_0$), then the distribution of the quasistatic fields is close to isotropic and condition 2) can not be satisfied.

[2)] We take the opportunity to point out that the statement made

in[21] that the central Stark components are shifted is incorrect. A detailed analysis shows that actually there is no shift of the central components. We note that footnotes 6 and 11 are also incorrect, and the factor $\gamma_l$ should be left out of formula (10) for the shift $D_\alpha^c$.

[3)] A detailed exposition of the theoretical questions considered below is contained in Chap. 3 of the dissertation[24], as well as in[25].

[4)] We have used here in place of $\alpha'$ the symbol $\alpha+u$, where $u$ is the energy difference between the sublevels $\alpha'$ and $\alpha$ in $\hbar\omega_F$ units.

[5)] By accident, the positions of a satellite shifted by $-3\lambda_p$ from a forbidden line in first interference order and of a satellite shifted from an allowed line by $4\lambda_p$ in second interference order coincide in this experiment.

[6)] Figure 4 shows a plot of $P(\mu)$ calculated for the case of isotropic distribution of the LF quasistatic fields. The previous measurements[5] have shown that the distribution of the LF noise is anisotropic: $(\langle E_\varphi^2\rangle)\approx(\langle E_r^2\rangle)\gg(\langle E_z^2\rangle)$. However, the degree of anisotropy of the LF noise, $\eta\equiv[\langle E_z^2\rangle/\langle E_\varphi^2\rangle]^{1/2}\approx 0.4$, differs inessentially from unity in order of magnitude. We can therefore expect that the anisotropy of the LF noise will not increase noticeably the 50% error in the measurement of $P(\mu)$.

[7)] This circumstance was pointed out to us by L. I. Rudakov.


[1]E. I. Kuznetsov and D. A. Shcheglov, Metody diagnostiki vysokotemperaturnoĭ plazmy (Methods of High-Temperature Plasma Diagnostics), Atomizdat, 1974, 3.3.

[2]G. V. Sholin, Dokl. Akad. Nauk SSSR **195**, 589 (1970) [Sov. Phys. Dokl. **11**, 1040 (1971)].

[3]E. A. Oks and G. V. Sholin, Zh. Tekh. Fiz. **46**, 254 (1976) [Sov. Phys. Tech. Phys. **21**, 144 (1976)].

[4]G. V. Sholin and E. A. Oks, Dokl. Akad. Nauk SSSR **209**, 1318 (1973) [Sov. Phys. Dokl. **18**, 254 (1973)].

[5]M. V. Babykin, A. I. Zhuzhunashvili, E. A. Oks. V. V. Shapkin, and G. V. Sholin, Zh. Eksp. Teor. Fiz. **65**, 175 (1973) [Sov. Phys. JETP **38**, 86 (1974)].

[6]Ya. F. Volkov, V. G. Dyatlov, and A. I. Mitina, Zh. Tekh. Fiz. **44**, 1448 (1974) [Sov. Phys. Tech. Phys. **19**, 905 (1974)].

[7]E. V. Lifshitz, Zh. Eksp. Teor. Fiz. **53**, 943 (1967) [Sov. Phys. JETP **26**, 570 (1968)].

[8]D. G. Yakovlev, Zh. Tekh. Fiz. **42**, 1557 (1972) [Sov. Phys. Tekh. Phys. **17**, 1248 (1972)]; A. E. Doltinov and D. G. Yakovlev, Astron. Zh. **50**, 1001 (1973) [Sov. Astron. **17**, 634 (1974)].

[9]S. H. Kim and H. E. Wilhelm, J. Appl. Phys. **44**, 802 (1973).

[10]H. G. Van Kampen, Physica (Utrecht) **74**, 215 (1974).

[11]A. Cohn, P. Bakshi, and G. Kalman, Phys. Rev. Lett. **29**, 324 (1972).

[12]P. Bakshi, G. Kalman, and A. Cohn, Phys. Rev. Lett. **31**, 1576 (1973).

[13]W. H. Rutgers and H. W. Kalfsbeck, Z. Naturforsch. Teil A **30**, 739 (1975).

[14]E. V. Lifshitz, A. B. Berezin, and Yu. M. Lyapkalo, Zh. Tekh. Fiz. **36**, 1087 (1966) [Sov. Phys. Tech. Phys. **11**, 798 (1966)]; I. A. Bez''yazychnyi, E. V. Lifshitz, A. K. Berezin, A. M. Artamonov, and A. V. Petukhov, in: Diagnostika plazmy (Plasma Diagnostics), **3**, Atomizdat, 1973, p. 59.

[15]A. B. Berezin, L. V. Dubovoĭ, B. V. Lyublin, and D. G. Yakovlev, Zh. Tekh. Fiz. **42**, 946 (1972) [Sov. Phys. Tech. Phys. **17**, 750 (1972)].

[16]C. C. Gallagher and M. A. Levine, Phys. Rev. Lett. **27**, 1693 (1971).

[17]W. R. Rutgers and H. de Kluiver, Z. Naturforsch. Teil A **29**, 42 (1974).

[18]L. P. Zakatov, A. G. Plakhov, V. V. Shapkin, and G. V. Sholin, Dokl. Akad. Nauk SSSR **198**, 1306 (1971) [Sov. Phys. Dokl. **16**, 451 (1971)].

[19]C. C. Gallagher and M. A. Levine, Phys. Rev. Lett. **30**, 897 (1973).

[20]C. C. Gallagher and M. A. Levine, J. Quant. Spectrosc. Radiat. Transfer **15**, 275 (1975).

[21]E. A. Oks and G. V. Sholin, Zh. Eksp. Teor. Fiz. **68**, 974 (1975) [Sov. Phys. JETP **41**, 482 (1975)].

[22]E. A. Oks and G. V. Sholin, Opt. Spektrosk. **42**, 761 (1977) [Opt. Spectrosc. (USSR) **42**, 434 (1977)].

[23]G. V. Sholin, A. V. Demura, and V. S. Lisitsa, Zh. Eksp. Teor. Fiz. **64**, 2097 (1973) [Sov. Phys. JETP **37**, 1057 (1973)].

[24]E. A. Oks, Candidate's Dissertation, Moscow Phys. Tech. Institute, 1975.

[25]A. I. Zhuzhunashvili and E. A. Oks, Preprint Inst. Atomic Energy-2836, 1977.

[26]K. Karplus and T. Schwinger, Phys. Rev. **73**, 1020 (1948).

[27]S. H. Authler and C. H. Townes, Phys. Rev. **100**, 703 (1955).

[28]C. H. Townes and A. L. Schawlow, Microwave Spectroscopy, McGraw, 1955.

[29]L. D. Landau and E. M. Lifshitz, Kvantovaya mekhanika (Quantum Mechanics), Fizmatgiz, 1963 [Pergamon 1968].

[30]M. Baranger and B. Mozer, Phys. Rev. **123**, 25 (1961).

[31]W. W. Hicks, R. A. Hess, and W. S. Cooper, Phys. Rev. **5**, 490 (1972).


Translated by J. G. Adashko